Proton-Conducting Polyhedral Oligosilsesquioxane Nanoadditives for Sulfonated Polyphenylsulfone Hydrogen Fuel Cell Proton Exchange Membranes

Claire Hartmann-Thompson,[1] Adrian Merrington,[1] Peter I. Carver,[1] Douglas L. Keeley,[1] Joseph L. Rousseau,[1] Dennis Hucul,[1] Kenneth J. Bruza,[1] Lowell S. Thomas,[1] Steven E. Keinath,[1] Robert M. Nowak,[1] Denise M. Katona,[2] Pasco R. Santurri[2]

[1]*Michigan Molecular Institute, Midland, Michigan 48640-2696*
[2]*Chemsultants International, 9079 Tyler Blvd., Mentor, Ohio 44060*

Received 2 January 2008; accepted 30 April 2008
DOI 10.1002/app.28665
Published online 10 July 2008 in Wiley InterScience (www.interscience.wiley.com).

ABSTRACT: Three novel polyhedral oligosilsesquioxane (POSS) nanofillers functionalized with proton-conducting sulfonic acid groups, mixed sulfonic acid and alkyl groups, and phosphonic acid groups were synthesized, characterized by IR, ^{1}H and ^{13}C NMR, and MALDI-TOF MS, and formulated into sulfonated polyphenylsulfone (S-PPSU) carrier polymers. High quality films were cast from 1-methyl-2-pyrrolidinone (NMP), and through-plane and in-plane proton conductivity, mechanical properties, water uptake, dimensional stability, and leaching behavior were measured to assess their suitability for use as hydrogen fuel cell proton exchange membranes. Various nanofiller loadings and S-PPSU sulfonation levels were studied. The morphologies of the composite membranes were determined by TEM and SEM X-ray mapping. When compared with Nafion®, the POSS-S-PPSU composite membranes exhibited comparable proton conductivity in combination with superior dimensional stability, heat resistance, and mechanical strength. When compared with control S-PPSU membranes, the composite POSS-S-PPSU membranes exhibited superior conductivity, comparable dimensional stability, and slightly decreased mechanical strength. © 2008 Wiley Periodicals, Inc. J Appl Polym Sci 110: 958–974, 2008

Key words: fuel cell; polyhedral oligosilsesquioxane; sulfonation; polyphenylsulfone; proton exchange membrane; composite; additives; ionomers; membranes; nanotechnology

INTRODUCTION

Many types of ion-conductive membranes have been developed for application in proton exchange membrane fuel cells.[1] The membrane must have the ability to transport protons from the anode to the cathode while simultaneously providing a barrier between the fuel (hydrogen or methanol) and the oxygen (or air) stream at the cathode. Membranes must also exhibit a good combination of chemical resistance, heat resistance, mechanical strength, ion conductivity, and low permeability to fuel crossover. Perfluorosulfonic acid ionomers such as Nafion® (DuPont, Wilmington, DE) and Flemion® (Asahi Glass, Tokyo, Japan) are highly conductive and chemically stable materials. However, they are costly to produce, lack mechanical strength and dimensional stability, have poor methanol crossover properties in direct methanol fuel cell applications, and perform poorly at the high temperatures necessary to achieve maximum catalyst efficiency (i.e., above 80°C). The other main class of ionically conductive polymers comprises aromatic polymers functionalized with sulfonic acid groups. Sulfonated polyaromatics are prepared either by postsulfonating an existing polymer or by reacting sulfonated monomers in condensation polymerizations.[1] As long as the sulfonation level and homogeneity of the product can be precisely controlled, and polymer chain scission can be avoided, the postsulfonation strategy is preferable,[2] since it requires only one reaction step, and can be carried out using a commercially available, cost-effective, and quality-consistent starting polymer. In contrast, many of the monomers used in the condensation polymerization strategy tend not to be commercially available and require single to multistep syntheses.

To address the shortcomings of conventional homopolymer fuel cell membranes, a number of composite membranes have been studied. Some composite membranes have interpenetrating network structures, e.g., polybenzimidazole (PBI) or polysulfone (PSU) interpenetrated with an ion-conducting material such as a sulfonated aromatic polymer or sulfonated fluoropolymer.[3,4] The Gore

Correspondence to: C. Hartmann-Thompson (thompson@mmi.org).

membrane is comprised of a Teflon® fluoropolymer film filled with an ion-conducting Nafion solution.[5] Other composite membranes are comprised of a proton conducting polymer and an inorganic additive. Both microscale additives (heteropolyacids,[6] zirconium phosphate,[7] calcium phosphate,[8] and silica,[9–13]) and nanoscale additives (titanium dioxide nanoparticles[14] and nanoscale silica[15–17]) have been studied extensively. In all of these membranes, the addition of inorganic fillers generally improves mechanical, dimensional, and thermal stability, and decreases methanol permeability in direct methanol fuel cells, but also results in decreased proton conductivity. This study explores the concept of improving composite fuel cell membrane performance without compromising proton conductivity by using a 1.5-nm closed-cage T8 polyhedral oligosilsesquioxane (POSS) form of nanosilica functionalized with proton-conducting sulfonic acid or phosphonic acid groups.

Two composite fuel cell membranes based on microscale additives carrying sulfonic acid groups have been reported. Sulfonic acid functionalized silica[18] (prepared by reaction with bis[3-(triethoxysilyl)-propyl] tetrasulfane and oxidation with hydrogen peroxide) was formulated into both sulfonated and nonsulfonated hydrogenated polybutadiene-styrene block copolymers,[19] and zeolites carrying sulfonated phenylethyl groups were formulated into Nafion.[20] Four composite fuel cell membranes based on silsesquioxanes have been reported. Polymethylmethacrylate or polystyrene copolymers with pendant POSS groups and proton-conducting polymers have been blended,[21] silsesquioxane resins have been added to sulfonated polyetheretherketone (S-PEEK),[22] and 10 nm to 10 μm MS64 and VTMOS polysilsesquioxane spheres[23] have been added to sulfonated polyethersulfone (S-PES)-S-PEEK blends.[24] A proton-conducting sulfonated bridged silsesquioxane membrane[25] was prepared by making a disulfide-functionalized xerogel membrane and postoxidizing the disulfide groups to sulfonic acid groups in nitric acid. A conductivity of 0.0062 S cm^{-1} was measured at ambient temperature and 100% RH.

However, only one other composite fuel cell membrane based on a sulfonated POSS has been reported.[26] An open-cage POSS carrying three glycidyl epoxy groups was reacted with 4-hydroxybenzenesulfonic acid, the resulting sulfonated POSS was blended with polyvinylalcohol and the blend was crosslinked using ethylenediaminetetracetic dianhydride (EDTAD). This system differs considerably from the system described in this study (open-cage versus closed-cage POSS, crosslinked versus non-cross-linked structure, aliphatic versus aromatic composition) and also has several disadvantages as follows: it requires a multistep fabrication process and it contains chemically unstable methylene groups. Additionally, the mechanical and chemical stability was not reported.

In this study, three closed-cage POSS nanoadditives carrying proton-conducting groups were synthesized, characterized, and formulated into a proton-conducting sulfonated aromatic carrier polymer. A postsulfonated polyphenylsulfone (PPSU), Solvay Radel® R-5000,[27,28] was selected as the carrier polymer. PPSUs are an attractive class of material because of their high mechanical, thermal, and chemical resistances, and commercial availability. Polyphenylsulfones (PPSU) have been postsulfonated using concentrated sulfuric acid,[28] sulfur trioxide in dichloromethane,[29,30] trimethylsilylchlorosulfonate (Me_3SiSO_3Cl) in dichloromethane,[29] chlorosulfonic acid in dichloromethane,[31] and sulfur trioxide-triethyl phosphate complex.[32] Polyethersulfones (PES), close relatives of PPSUs, have been postsulfonated using concentrated sulfuric acid,[33] a solution of chlorosulfonic acid in sulfuric acid,[34–36] a slurry of chlorosulfonic acid in dichloromethane,[37–39] chlorosulfonic acid in combination with a carboxylic anhydride,[40] sulfur trioxide in dichloromethane,[41] and sulfur trioxide-triethyl phosphate complex.[42,43] Surface sulfonations of PES and PPSU membranes have been carried out using sulfur trioxide in the gas phase.[44] In this study, sulfonation was carried out using a chlorosulfonic acid-carboxylic acid anhydride method.[40] Thirty years ago, the sulfonation of a PPSU was reported for a reverse osmosis application,[45] and since then sulfonated PES and sulfonated PPSU have been used for pervaporation membranes,[43] ultrafiltration membranes,[33,38] dialysis membranes,[31] nanofiltration membranes,[33,39,46] and microcellular foams.[32] The comparatively novel engineering thermoplastic, polyethersulfone Cardo (PES-C, carrying a five-membered lactone ring derived from phenolphthalein),[47] has also been sulfonated using concentrated sulfuric acid at room temperature and assessed as a direct methanol fuel cell membrane. Other variants of sulfonated polyphenylsulfone (S-PPSU) and S-PES fuel cell membrane materials include block copolymers,[48] blends with polybenzimidazole (PBI),[49] phosphonated PPSU,[50] mixed sulfonated/phosphonated PPSU,[50] and mixed sulfonic acid/$SiPh(OH)_2$ PPSU.[51]

EXPERIMENTAL

Materials

Octaphenyl POSS was obtained from Hybrid Plastics (Fountain Valley, CA). PPSU (Radel R-5000) was obtained from Solvay Advanced Polymers (Alpharetta, GA). Two batches of S-PPSU were obtained from Akron Polymer Systems, (Akron, OH) and the other S-PPSU batches used in this study were

prepared as described. Organic reagents were obtained from Sigma-Aldrich (Milwaukee, WI) and used as received.

Chemical characterization

IR spectra were recorded using a Nicolet 20DXB FTIR spectrometer using samples cast from solution onto potassium bromide disks. The IR spectra of less soluble compounds were recorded in the solid state using a Nicolet Nexus 670 FTIR diamond ATR instrument. ^{1}H NMR spectra were recorded on a Varian 400-MHz NMR System spectrometer equipped with a 5-mm broad band probe. Solvent signals were used as internal standards, and chemical shifts are reported relative to tetramethylsilane (TMS). MALDI-TOF mass spectra were measured by M-Scan (West Chester, PA) using an Applied Biosystems Voyager DE-Pro instrument. Size exclusion chromatography multi-angle laser light scattering (SEC-MALLS) molecular weight distribution parameters were measured using an Agilent 1050 system (pump, autosampler, and UV detector), a Waters 2410 DRI detector, and a Wyatt Dawn EOS (690 nm) multi-angle laser light scattering detector. The eluant was 0.05% lithium bromide in NMP. Narrow polystyrene (50 kD) was used to normalize the various detectors used. Two Polymer Laboratories PLgel columns (65°C) were used to separate the samples based on size. Samples were dissolved in eluant by heating at 130°C overnight followed by low shear mixing for several hours.

Preparation of nanoadditives

Sulfonic acid POSS (designated S-POSS)

Octaphenyl-POSS (69.8 g, 67.5 mmol) was added to chlorosulfonic acid (250 mL, 3.76 mol). The reaction solution was stirred overnight at room temperature. Unreacted chlorosulfonic acid was removed by vacuum distillation. Deionized water (400 mL) was added to dissolve the crude product. The volume was reduced to 100 mL under reduced pressure. The crude product was washed three times with anhydrous tetrahydrofuran (1.5 L). The product was then dried under reduced pressure to give a brown solid in quantitative yield. IR: ν (cm^{-1}): 3070 (OH of SO_3H), 2330 ($SO_3H—H_2O$), 1718, 1590, 1470, 1446, 1395, 1298, 1132 (SO_3 asym), 1081 (SO_3 sym), 1023 (SiOSi asym), 991, 806 (SiOSi sym); ^{1}H NMR (D_2O): δ_H (ppm) 7.54 (dd; Ar*H meta* to POSS), 7.81–7.83 (2dd; Ar*H para* to SO_3H, Ar*H para* to POSS), 8.03 (dd; Ar*H ortho* to SO_3H and POSS); ^{13}C NMR (D_2O): δ_C (ppm) 122.5 (ArCH), 128.4 (ArCH), 130.0 (ArCH), 143.2 (ArCH); MALDI-TOF MS: *m*/*z* 1698 (Calc. 1697, molecular ion plus sodium).

Alkylated POSS (designated A-POSS)

1-Chlorooctadecane (169.8 g, 0.587 mol) in solution with dichloromethane (600 mL) was mixed under nitrogen with octaphenyl POSS (76.45 g, 74.0 mmol). Aluminum chloride (20 g, 15 mmol) was added in four parts over a 10-min period. The mixture was stirred initially at 0°C and allowed to warm to room temperature over 3 days; 100 mL of water was added, resulting in a pale precipitate. The crude product was extracted into ethyl acetate from water. The ethyl acetate was removed under reduced pressure. THF was used to dissolve the crude product, which was filtered through a short column of flash silica. The volume of the filtered solution was reduced to about 100 mL and the solution was precipitated into acetone (1.5 L). The acetone solution was decanted off and discarded. Chloroform was used to dissolve the material, which was dried under reduced pressure to produce oil. Yield: 154.2 g, 68%. ^{1}H NMR (D_2O): δ_H (ppm) 0.87 (t; C*H*$_3$), 1.42 (m; C*H*$_2$), 7.01 (s; Ar*H ortho* to POSS), 7.11 (m; Ar*H-meta* to POSS), 7.56, and 7.67 (m; Ar*H ortho* and *para* to POSS). ^{13}C NMR (D_2O): δ_C (ppm) 19.7 (*C*H$_3$), 26.1 to 31.8 (various *C*H$_2$), 37.1 (Ar*C*H$_2$), 127.2 (Ar*C*H), 130.2 (Ar*C*H), 131.7 (Ar*C*H) 133.6 (Ar*C*H). MALDI-TOF MS: (*m*/*z*) 2820 (Calc. 2820, hepta-substituted POSS, molecular ion plus sodium) 3072 (Calc. 3073, octa-substituted POSS, molecular ion plus sodium).

Sulfonic acid alkylated POSS (designated SA-POSS)

Alkylated POSS (73.31 g, 24.3 mmol) was dissolved in dichloromethane (300 mL) and cooled in an ice-water bath. Sulfuric acid (21 g, 11 mL, 0.214 mol) was added to the solution and stirred overnight at room temperature. Dichloromethane was removed under reduced pressure and the resulting oil was added to dry methanol (1.2 L) and formed a precipitate. The precipitate was dissolved in chloroform and then dried under reduced pressure. Yield = 75.81 g, 82%. IR: ν (cm^{-1}) 3068, 3049, 3005 (ArH), 2951, 2924, 2843 (CH_2 and CH_3), 2726, 2676 ($SO_3H—H_2O$), 1681, 1596, 1429 (Si-Ph, sym) 1378, 1156 (SO_3 asym), 1118 (SiOSi asym), 788 (SiOSi sym). ^{1}H NMR (D_2O): δ_H (ppm) 0.86–0.90 (t; C*H*$_3$), 1.27–1.40 (m; C*H*$_2$), 1.52–1.59 (m; C*H*$_2$), 2.48 (C*H*$_2$Ar), 7.05–7.81 (3m; Ar*H*), 9.54, and 11.05 (SO_3H). ^{13}C NMR (D_2O): δ_C (ppm) 14.5 (*C*H$_3$), 20.1 to 32.6 (various *C*H$_2$), 37.4 (Ar*C*H$_2$), 127.3 (Ar*C*), 128.5 (Ar*C*H), 132.1 (Ar*C*H), 133.4 (Ar*C*), 134.0 (Ar*C*), 134.7 (Ar*C*H).

Phosphonic ester POSS (designated PE-POSS)

Octabromophenyl POSS[52] (87.09 g, 5.3 mmol) was dissolved in tetrahydrofuran (1000 mL) and cooled

TABLE I
Reaction Conditions, Sulfonation Levels, and Molecular Mass Data for Sulfonated PPSU Batches 1 to 8 in Order of Decreasing Sulfonation Level

	Radel® R-5000 PPSU (g)	CH_2Cl_2 (mL)		$ClSO_3H$ (mL)	Ac_2O (mL)	Total time (h)	DS	wt % SO_3H	M_w	M_n	M_w/M_n
1	50	300	360	20	6	6.75	81.7	27.2	66,440	42,060	1.58
2	–	–	–	–	–	–	75.4	23.5	–	–	–
3	50	300	360	16	6	6.5	64.1	20.7	42,200	31,230	1.35
4	50	300	360	20	6	6.75	70.3	22.2	44,700	32,610	1.37
5	100	600	700	32	10	6.5	64.5	21.5	30,200	22,340	1.35
6	–	–	–	–	–	–	58.5	19.2	–	–	–
7	50	300	300	8.75	10	2.75	26.4	9.7	47,340	36,980	1.28
8	20	140	140	3	5	4	20.0	7.5	40,540	29,730	1.36

Compounds **2** and **6** were obtained from an external supplier. The double entries in the CH_2Cl_2 column correspond to the volume used to prepare the initial PPSU solution and the volume used to dilute the initial solution.

to −78°C in a dry-ice slush bath. Butyl lithium (27.45 g, 0.429 mol) was added to the solution followed by diphenylchlorophosphate (115.4 g, 0.429 mol). The solution was allowed to warm to room temperature overnight. Deionized water (200 mL) was added and the solvents were removed under reduced pressure. The crude product was washed three times with water (200 mL) and then with hexane (200 mL). The product was dried under reduced pressure. Yield = 118 g, 78%. ^{1}H NMR ($CDCl_3$): δ_H (ppm) 7.2 (m; Ar*H*). ^{13}C NMR ($CDCl_3$): δ_C (ppm) 120.1 (POAr*C*H), 125.1 (POAr*C*H), 127.9 (POSSAr*C*H), 129.6 (POAr*C*H), 134.1 (POSSAr*C*H), 150.5 (s; POAr*C*O). MS (MALDI-TOF): *m*/*z* 1287 (Calc. 1287 monosubstituted molecular ion + Na, $POSSPh_7(Ph(PO(OPh)_2)$, 1543 (Calc. 1543 disubstituted molecular ion + 2Na, $POSSPh_6(Ph(PO(OPh)_2)_2)$, 2258 (Calc. penta-substituted 2253 molecular ion + 5Na, $POSSPh_3(Ph(PO(OPh)_2)_5)$.

Phosphonic acid half ester POSS (designated P-POSS)

Hydrolysis of the diphenyl phosphonic acid ester was performed using a two-phase solution of tetrahydrofuran (200 mL), sodium hydroxide (75 g, 1.9 mol), and deionized water (150 mL). The mixture was stirred for 2 days and then allowed to separate. The organic layer was decanted off and dried. Concentrated hydrochloric acid (200 mL, 37 wt %) was added to the crude product and stirred overnight. The acid was decanted off, the product dissolved in acetone (100 mL) and the solution was filtered. The product was then dried under reduced pressure. Yield = 12 g. IR: ν (cm^{-1}) 3067 (ArH), 3040 (ArH), 2700 (POH), 2100 (POH), 1630 (HOP=O), 1584, 1487, 1196 (SiOSi asym), 1087 (P=O) 944 (POH, str), 753 (SiOSi sym). ^{1}H NMR (CD_3OD): δ_H (ppm) 6.87–6.91 (m; Ar*H*), 6.95–6.97 (m; Ar*H*), 7.05–7.10 (m; Ar*H*). ^{13}C NMR (CH_3OD): δ_C (ppm) 120.5 (POAr*C*H), 122.7 (POSSAr*C*H), 124.7 (POAr*C*H), 127.8 (POSSAr*C*H), 129.9 (POAr*C*H), 133.9 (POSSAr*C*H), 152.4 (POAr*C*O).

Preparation of sulfonated polyphenylsulfone

Reaction conditions used in the preparation of S-PPSU batches **1** to **8** are summarized in Table I. A preparation of S-PPSU is given as an example.

Sulfonated polyphenylsulfone 1

Radel R-5000 PPSU was dried for 24 h at 140°C. Dried PPSU (50 g) was added to dichloromethane (300 mL) and mixed for 12 h. An additional 360 mL of dichloromethane was added and the solution was transferred to a clean glass beaker. The beaker was placed in an ice bath on a stirring plate and the solution was cooled to 10°C under agitation. Chlorosulfonic acid (20 mL) was added dropwise over a 1h period while stirring continuously. Acetic anhydride (6 mL) was added dropwise to the mixture. The reaction was then allowed to proceed for a period of 6.75 h while stirring and maintaining the temperature between 5 and 10°C. The reaction was stopped by gradually pouring the reacted solution into an ice-deionized water mixture. The resulting precipitate was recovered by decanting and washed repeatedly with deionized water until the wash water was shown to have a pH of 5–6. The sulfonated polyphenylsulfone (S-PPSU) was subsequently dried for 72 h at 60°C. ^{1}H NMR (d_6-DMSO): δ_H (ppm) 6.96–6.99 (d; Ar*H*, sulfonated biphenyl, *ortho* to O), 7.05–7.24 (2m; Ar*H*, nonsulfonated biphenyl, *ortho* to O, Ar*H*, SO_2Ph, *meta* to SO_2), 7.64–7.72 (m; Ar*H*, sulfonated and nonsulfonated biphenyl, *meta* to O), 7.83–7.85 (dd; Ar*H*, sulfonated biphenyl, *ortho* to SO_3H), 7.90–7.93 (m; Ar*H*, SO_2Ph *ortho* to SO_2), 8.05 (d; SO_3H).

Calculation of degree of sulfonation

The degree of sulfonation (DS) was determined via calculation from integral values for peaks in the aromatic region of the ^{1}H NMR spectrum. In many literature PPSU and PES sulfonation studies, only one position per polymer repeat unit is readily

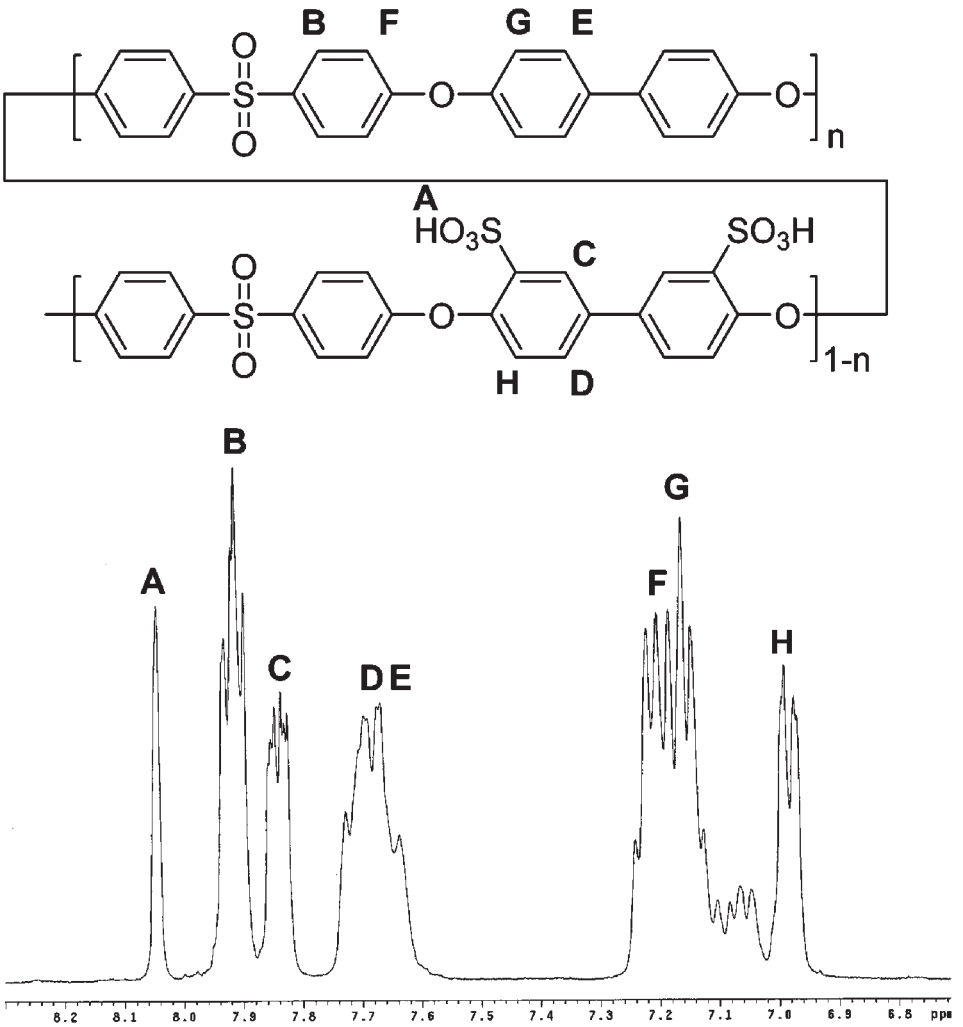

Figure 1 ^{1}H NMR of S-PPSU.

sulfonated under normal conditions and able to carry a sulfonic acid group, and the ^{1}H NMR DS calculation is straightforward.[34] In this case, the situation is more complicated because two possible positions may be sulfonated in the electrophilic sulfonation of the Radel R-5000 S-PPSU repeat unit (Fig. 1). Hence a distribution of repeat units carrying two sulfonic acid groups, one sulfonic acid group, or no sulfonic acid groups is possible. In this study, the DS value is defined as the percent of biphenyl-type single phenyl rings that carry one sulfonic acid group and is calculated from the integral corresponding to the protons *meta* to oxygen in both a sulfonated and a nonsulfonated biphenyl unit (7.6–7.8 ppm, positions D and E in Fig. 1) and the integral corresponding to a sulfonated biphenyl-type single phenyl ring (one proton *ortho* to SO_3H at 7.8 ppm, position C in Fig. 1). This DS value is only equal to the true fraction (percent) of polymer repeat units sulfonated if a hypothetical structure is assumed in which a nonsulfonated repeat unit carries no sulfonic acid groups, and a sulfonated repeat unit carries two sulfonic acid groups in two *ortho* to oxygen positions on each ring of the two-ring biphenyl unit. The NMR assignments given in Figure 1 follow those given for a literature sulfonated polyphenylenesulfide sulfone with a substitution pattern identical to the hypothetical S-PPSU described earlier,[53] and also for a brominated S-PPSU.[54] It should be noted that an earlier literature ^{1}H NMR spectrum of sulfonated Radel R-5000 PPSU was mis-assigned and failed to take the possibility of one versus two sulfonic acid groups per single polymer repeat unit into account.[29]

A weight percent (wt %) content of sulfonic acid groups can be readily calculated from the DS value. Obviously the wt % of sulfonic acid groups will be the same regardless of how the sulfonic acid groups are distributed across polymer repeat units and along the polymer chain (i.e., the zero versus one versus two sulfonic acid group distribution alluded to above).

Calculation of ion exchange capacity

The ion-exchange capacity (IEC, defined as the number of milliequivalents of ions in 1 g of dry polymer)[36] was determined via a titration method. A known weight (0.2–0.4 g) of the dry polymer was placed in 50 mL of a 2.0*M* NaCl solution and kept at 40°C for 24 h. The solutions were shaken occasionally to allow for complete release of H^+ ions. A 10-mL sample was removed from the solution and titrated with 0.01*M* NaOH solution using bromothymol blue indicator. The ion-exchange capacity was determined using eq. (1).

$$\mathrm{IEC\,(mmoL\ g^{-1})} = 0.05 \times V\,(\mathrm{mL})/W\,(\mathrm{g}) \qquad (1)$$

where V is the volume of titrant used in mL and W is the weight of the dry polymer sample in g. Three replicates of each sample were tested and the results averaged. The standard deviation was 0.03 mmol g^{-1}.

S-PPSU membrane preparation

S-PPSU polymer was dissolved in NMP at 20% by weight solids, and the resulting solution was filtered through a 25 micron mesh filter. The solution was cast onto a clean glass plate using a film applicator. An appropriate gap setting was used to produce a 50-μm dry film. The cast membrane was dried in a 140°C oven for 30 min, cooled for 15 min and subsequently removed from the glass plate. Analytical results showed that residual NMP solvent in the laboratory cast films was below 0.28 wt %.

S-PPSU-POSS membrane preparation

Films were cast from a 20 wt % solids NMP solution as described earlier. The 20 wt % solids solution was prepared by first grinding the POSS nanoadditive and dissolving in water at 80°C, combining the NMP and water solutions, and then removing water in an oven (100°C in air). This predispersed solution of POSS in NMP was added to predissolved S-PPSU in NMP to give the desired 20 wt % solids solution.

Membrane electrode assembly preparation

Prior to membrane electrode assembly (MEA) preparation, membranes were put through a cleaning process involving boiling in 3% hydrogen peroxide, followed by boiling in deionized water, followed by boiling in 1.0*M* sulfuric acid, followed by further boiling in deionized water. MEAs consisting of a 5 cm^2 active area centered on 58 cm^2 membrane were prepared as follows. A catalyst ink solution was made using 0.020 g of 20% platinum/carbon catalyst (Vulcan XC-72), 0.080 g of a 10% Nafion solution (Fuel Cell Store Nafion Solution DE1021), and 0.265 g of isopropanol (Fisher Scientific A416-20). After thorough mixing, half of this solution was added to one gas diffusion layer (GDL) and the other half to a second GDL, where 2.5 cm square pieces of ELAT cloth were used as GDLs (Fuel Cell Store GDL LT 1200-W). After drying overnight in a fume hood, the pair of coated GDL's were placed on opposite sides of a membrane that was 7.6 cm on each side. This assembly was placed between two Teflon-coated fiberglass backed Viton press pads. The entire assembly was placed in a preheated hydraulic press (Pasadena Hydraulics Model PW-2270) at 80°C at a pressure of 1500 pounds per square inch. The assembly was held at constant pressure for 5 min at 80°C and then cooled to room temperature, maintaining constant pressure during cooling. The MEA was then used in the fuel cell test stand without additional treatments.

Conductivity

Through-plane conductivities of the membranes were measured at 70°C and 80% RH by electrochemical impedance spectroscopy (EIS) using Fuel Cell Technologies (FCT) Dual Channel Fuel Cell Test Station (Albuquerque, NM) fitted with a single cell AC-*Z* impedance unit. Conductivity values were obtained from the bulk specimen resistance R as Z' (real component of AC impedance) tended to a minimum at infinite frequency. A standard deviation of 0.005 S cm^{-1} was obtained when repeat experiments were performed. A MEA was placed inside a 5 cm^2 FCT Fuel Cell Hardware Assembly (cell). The cell consisted of a pair of Poco Graphite blocks with a precision-machined, single-serpentine flowpattern, a pair of gold-plated connectors fastened with aluminum endplates, gas inputs, and outputs through Swagelok® fittings, a thermocouple well and two cartridge heaters. The cell temperature was monitored by a thermocouple. The MEA comprises five layers: a central polymer electrolyte membrane (PEM) sandwiched between two electrode/catalyst layers supported on carbon cloth. The MEA was housed within the cell using Teflon-coated fiberglass gaskets. Zero-grade hydrogen was used at the anode side, zero-grade oxygen was used at the cathode side, and zero-grade nitrogen was used to flush the system prior to evaluation. Gas flow was controlled by a series of mass flow controllers. The gases were humidified to near dew point using FCT Hi-Flow Rate Humidity Bottle Assemblies with Auto-Fill (HB/AF) capabilities set at a temperature of 70°C.

In-plane conductivity measurements of the cast membranes were obtained using an Agilent Milliohmmeter type 4338B AC impedance meter with a test frequency of 1 kHz. An open-frame cell with two platinum electrodes was used. The membranes were first treated in a 1.0*M* H_2SO_4 solution for several hours at room temperature and then subsequently washed with deionized water for several additional hours. The conductivity of the membranes was measured in the lateral (in-plane) direction while still in the fully hydrated state.

Water uptake

Test sample membranes were soaked in deionized water for 24 h at 80°C. The liquid water on the surface of the wetted membranes was blotted off with a laboratory tissue prior to weighing. The samples were then dried for 48 h at 100°C and weighed again. The amount of water uptake in the membranes was calculated [eq. (2)]. This technique gave a standard deviation of 3.5%.

$$\text{Water uptake}\,(\%) = [(\text{wet weight} - \text{dry weight})/\text{dry weight}] \times 100 \quad (2)$$

Dimensional stability

ASTM Test D 1042-01a (Standard Test Method for Linear Dimensional Changes of Plastics under Accelerated Service Conditions) was followed to measure dimensional changes in films after exposure to specified humidity environments. Samples were equilibrated for 24 h in the laboratory at room temperature, inscribed with an arc, exposed to the test conditions and then re-inscribed. The difference between the two arcs was measured with the aid of a microscope, and expansion (or contraction) of the film was quantified as a percent of linear change, L_C, where D_B is the distance between the inscribed arcs, and D_I is the initial inscribed distance [eq. (3)]. When repeat experiments were performed, standard deviations of 0.5 to 1% were obtained. A 100% RH test environment was obtained using a 1% aqueous sulfuric acid solution, a 52% RH test environment was obtained using a saturated $NaHSO_4$-H_2O solution,[55] and anhydrous conditions were obtained using an oven at 80°C.

$$L_c = D_B/D_I \times 100 \quad (3)$$

Mechanical and thermal analyses

The tensile strength properties of the cast membranes were determined using a ChemInstruments TT-1000 tensile tester equipped with a 25-pound (111.2 N) load cell. The test speed was set to a rate of 50 mm per minute. The cross-sectional area of the membrane samples was measured before testing and the gauge length between the grips was 50 mm. The tensile strength to break was calculated according to eq. (4).

$$\text{Tensile strength}\,(\text{N/mm}^{-2}) = \text{Maximum load}\,(\text{N})/\text{cross-sectional area}\,(\text{mm}^2) \quad (4)$$

Three test specimens were tested for each membrane sample and the results were averaged. A standard deviation of 1.35 N mm^{-2} was obtained for tensile strength and a standard deviation of 4.7% was obtained for elongation.

DMA measurements were made using a TA Instruments Model 2980 Dynamical Mechanical Analyzer with film tension fixture. The DMA measurements were controlled by TA Instruments Thermal Solutions software. The data were analyzed with TA Instruments Universal Analysis V4.1 to determine the storage modulus E', loss modulus E'', and tan $\delta = E''/E'$. E' is the in-phase, elastic component, and E'' is the out-phase, viscous component, and tan $\delta = E''/E'$. Heating scan experiments were carried out over a temperature range of 30–220°C at a scan rates of 2°C min^{-1}, and at an oscillation frequency of 1 Hz with 25 μm amplitude. The purge (bearing) gas employed was air. The sample was rectangular with length of $\sim$ 24 mm. The width was $\sim$ 7 mm as measured by a caliper.

Microscopy

A small specimen was cut with a razor blade from a representative area of each sample and clamped in the specimen chuck of the Leica Ultracut UCT ultramicrotome with EMFCS cryo attachment. Specimens were cooled to −100°C. Cooled specimens were trimmed and faced, and then cross-sectioned with the ultramicrotome set for 90-nm sectioning thickness. Sections were collected onto clean copper mesh TEM specimen grids. Grids were examined in a Hitachi H-600 TEM at an accelerating voltage of 100 kV. Digital images were collected at a range of magnification settings with a Gatan MultiScan Model 794 digital camera.

Scanning electron microscope (SEM) with X-ray mapping for silicon was carried out using an Amray 1820 SEM with a lanthanum hexaboride electron source, equipped with EDAX Genesis instrumentation for energy dispersive spectroscopy (EDS). The film was cryo-fractured in liquid nitrogen, and the resulting film was mounted on a SEM stub and coated with carbon in a vacuum evaporator to control charging. The fracture surface was examined at

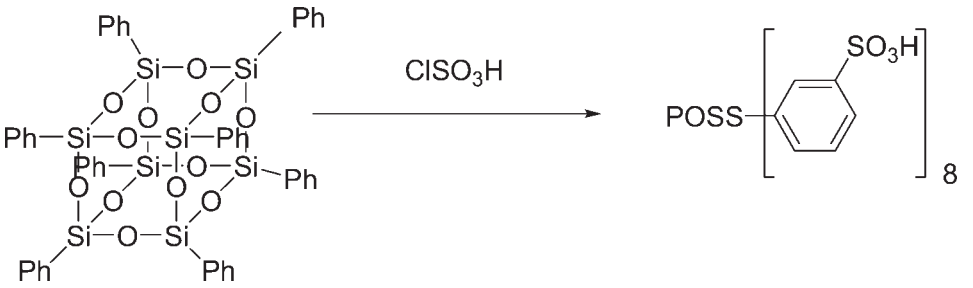

Scheme 1 Preparation of S-POSS.

5 kV to produce SEM images, and an X-ray map was produced.

RESULTS AND DISCUSSION

Preparation and characterization of POSS nanoadditives

Sulfonic acid POSS (S-POSS) was prepared in a one-step aromatic electrophilic sulfonation of octaphenyl POSS using an excess of chlorosulfonic acid (Scheme 1), and the resulting brown solid was characterized by IR, ^{1}H NMR, ^{13}C NMR, and MALDI-TOF mass spectrometry. The asymmetric SO_3 band at $\sim$ 1150 cm^{-1} and the symmetric SO_3 band between 1000 and 1100 cm^{-1} characteristic of aromatic sulfonic acids[39] were observed in the IR spectrum. An asymmetric SiOSi band at $\sim$ 1050 cm^{-1} and a symmetric SiOSi band at $\sim$ 800 cm^{-1} associated with POSS were also observed. The S-POSS compound had markedly different solubility characteristics to the starting octaphenyl POSS reagent. S-POSS was soluble in water, whereas octaphenyl POSS was not. Four peaks were observed in the aromatic region of the ^{1}H NMR spectrum with chemical shifts, integrals, doublets, and coupling constants consistent with the four nonequivalent protons of a *meta*-disubstituted phenyl group carrying a sulfonic acid group, and the electron-withdrawing and *meta*-directing POSS substituent. Four strong ArCH peaks were also observed in the aromatic region of the ^{13}C NMR spectrum. In contrast, the starting octaphenyl POSS reagent is a mono-substituted phenyl compound with three nonequivalent aromatic proton environments and three nonequivalent ArCH carbon environments.

To study the effect of long (C_{18}) alkyl chains on the solubility of sulfonated POSS, and on the additive dispersion and morphology of an S-PPSU-POSS membrane, a POSS compound carrying both C_{18} alkyl groups and sulfonic acid groups was prepared in a two-step synthesis (Scheme 2). In the first step, octaphenyl POSS was alkylated in a Friedel-Crafts reaction. Initially, a literature method for the Friedel-Crafts alkylation of benzene with *t*-butyl chloride and aluminum chloride at 0°C was used[56] but ^{1}H NMR showed that only one-third of the POSS phenyl groups had been successfully alkylated. The method was then modified. The molar excess of aluminum chloride to octaphenyl POSS was increased from 1.5-fold to fivefold, the reaction time was extended from a few minutes to 3 days, the temperature was raised from 0°C to room temperature, and a fully alkylated product was obtained. The MALDI-TOF mass spectrum of this material had a distribution of peaks at 252 mass unit intervals (corresponding to the octadecyl group). The peak at the center of the distribution with the highest intensity was at 2820, corresponding to a structure with seven alkyl groups per POSS (target mass of 2797 plus sodium). The high mass side of the distribution went up to 3575, corresponding to a structure with 10 alkyl groups per POSS (target mass of 3552 plus sodium)

Scheme 2 Preparation of SA-POSS.

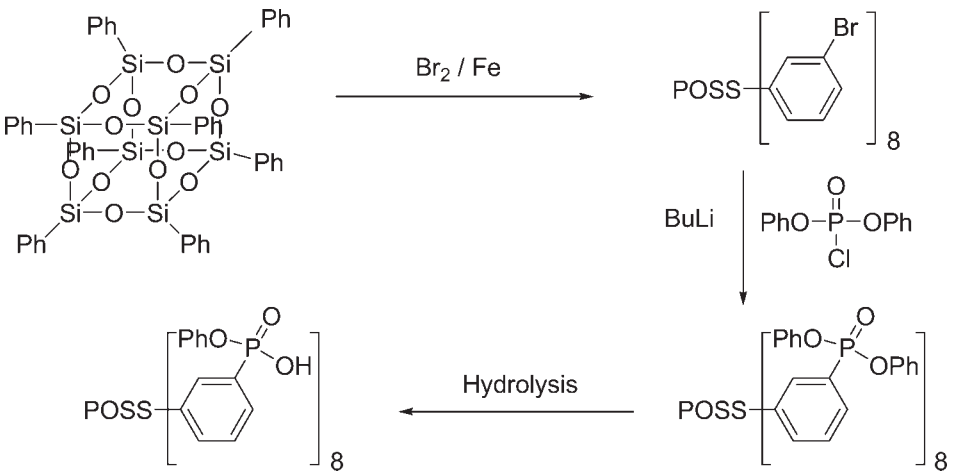

Scheme 3 Preparation of P-POSS.

and demonstrating that a small fraction of the phenyl rings had been dialkylated. The ^{1}H and ^{13}C NMR spectra suggested *meta*-substitution had occurred as expected. This material had good solubility in chloroform.

In the second step, the A-POSS product was sulfonated using sulfuric acid in dichloromethane. Since alkylated octaphenyl POSS is more activated to electrophilic aromatic substitution than octaphenyl POSS (because of the inductively electron-donating nature of the alkyl group), a more mild sulfonating system than the chlorosulfonic acid used earlier for octaphenyl POSS was selected. In the SA-POSS IR spectrum, SO_3 and SiOSi bands were observed (as per the S-POSS discussion earlier) plus methyl and methylene symmetric and asymmetric stretch bands in the 2800–2900 cm^{-1} region associated with the octadecyl groups. The ^{1}H and ^{13}C NMR spectra suggested that trisubstituted phenyl groups were present (i.e., carrying a POSS, an alkyl, and a sulfonic acid group). There were three peaks in the aromatic region of the ^{1}H NMR spectrum corresponding to three nonequivalent aromatic proton environments, and three strong peaks in the aromatic region of the ^{13}C NMR spectrum corresponding to three nonequivalent ArCH carbon atoms. However, the spectra did not contain sufficient information to determine whether the sulfonic acid groups were *ortho* or *para* (or both) to the POSS substituent; this material was water-soluble.

Phosphonic acid half ester POSS (P-POSS) was prepared in a three-step synthesis (Scheme 3). In the first step, octaphenyl POSS was brominated using bromine and iron in a literature method described elsewhere.[52] The NMR and mass spectra showed that the desired product had been obtained. In the second step, octabromophenyl POSS was phosphonated[57,58] using diphenylchlorophosphate and butyl lithium under the rigorously anhydrous and oxygen-free conditions necessary for the use of pyrophoric reagents. The MALDI-TOF mass spectrum showed a distribution of products ranging from a POSS carrying one phosphonic ester group to a POSS carrying five phosphonic ester groups. This material was soluble in chloroform. In the third step, PE-POSS was then hydrolyzed to the desired phosphonic acid half ester P-POSS product following a literature method using sodium hydroxide in THF,[59] which was subsequently modified and found to give improved yields if wet THF was used and/or water was added to anhydrous THF. The expected asymmetric and symmetric POSS bands were observed in the IR spectrum, plus a number of bands characteristic of a phosphonic acid half ester,[60] i.e., a POH stretch band at 944 cm^{-1}, a P=O stretch at 1087 cm^{-1}, acid salt bands at 2700 and 2100 cm^{-1}, and a distinctive HOP=O band at 1630 cm^{-1} associated with species in which one P=O is combined with one POH (such as phosphonic acid half esters, phosphinic acids, or phosphonous acids). Since both the phosphonic ester precursor (PE-POSS) and the phosphonic half-ester product (P-POSS) contain disubstituted POSS phenyl groups and phosphonic ester phenyl groups, the ^{1}H and ^{13}C NMR spectra of these materials were very similar and the aromatic regions were complex because of the presence of numerous aromatic protons and carbon atoms. However, it was possible to assign the spectra using the ^{1}H and ^{13}C NMR spectra of the model compounds diphenylphosphate and triphenyl phosphate[61] to distinguish POSS-aromatics from P-O-aromatics. P-POSS was soluble in methanol.

Preparation and characterization of sulfonated PPSU

The reagents and conditions for the preparation of eight batches of S-PPSU are summarized in Table I.

TABLE II
IEC, Water Uptake, and Conductivity Data for Sulfonated PPSU Materials 1 to 8 in Order of Decreasing Sulfonation Level

S-PPSU	IEC (mmol g^{-1})	Degree of sulfonation (DS, %)	Water uptake (%)	Conductivity (S cm^{-1})	
				Through-plane/70°C	In-plane/RT
1	1.81	81.7	224	0.110	0.086
2	1.57	75.4	90	0.036	0.069
3	1.67	64.1	53	0.065	0.049
4	1.55	70.3	54	0.038	0.058
5	1.56	64.5	42	0.036	0.040
6	1.20	58.5	40	0.020	0.020
7	0.85	26.4	19	0.000	0.002
8	0.25	20.0	14	0.000	0.001

Batches **2** and **6** were obtained from an external supplier. A chlorosulfonic acid-acetic anhydride sulfonation system was used.[40] As described elsewhere, the DS can be controlled by reaction time and temperature in chlorosulfonic acid[35] sulfonations and also in other sulfonating systems such as concentrated sulfuric acid.[33] In this series of eight reactions, the same temperature was used but reaction times and reagent ratios were varied (Table I). If reaction temperature goes above a certain threshold or reaction times are too long, chain scission is common in postsulfonation of PPSU and PES.[2,33,35,39] To check that chain scission was not occurring, SEC in NMP was run on six of the S-PPSU batches, and the molecular masses obtained were higher than those obtained for a control sample of Radel R-5000 PPSU run under identical SEC conditions (M_w = 32,670; M_n = 20,660; M_w/M_n = 1.58). The phenomenon of chain scission may also be studied by UV spectroscopy, where the presence of a maximum at 321 nm has been attributed to the formation of phenol end-groups at points where the chain has been cleaved.[33] In this study, the DS was measured directly by ^{1}H NMR, although DS has also been determined by quantitative FTIR on the SO_3Na IR band[33] at 1040 cm^{-1}. Postsulfonation of PES and PPSU polymers is known to increase the glass transition temperature (T_g) relative to the nonsulfonated starting materials,[33,35] and DSC confirmed that T_g also increased in this system. The starting Radel *R*-5000 PPSU had a T_g of 222°C, whereas S-PPSU **3** had a T_g of 229°C.

Preparation and characterization of S-PPSU membranes

To study the properties of the eight batches of S-PPSU and to select the optimum carrier polymer for the proton-conducting POSS nanoadditives, S-PPSU films were cast from 20 wt % solids NMP solutions, and IEC, water uptake, and through-plane and in-plane proton conductivity measurements were made (Table II). The IEC of a material, defined as the number of milli-equivalents of ions in 1 g of dry polymer,[36] gives information about the DS of a material. Although IEC generally increases with increasing DS (Table II), it should be noted that NMR DS values seldom match DS values calculated from IEC titration results.[34,53] This has been attributed to the fact that the NMR DS value is a direct measurement of the chemical composition of the polymer, whereas IEC is an indirect titration measurement dependent upon interaction between hydroxide ions and sulfonic acid groups, and that such interactions are affected by polymer microstructure.[53] In this study, when wt % SO_3H was calculated from the IEC value, it was lower than the wt % SO_3H value obtained from the ^{1}H NMR DS. For example, ^{1}H NMR shows that Batch **1** contains 27.2 wt % SO_3H (Table I), whereas the IEC value shows that Batch **1** contains 1.81 mmol of ions per gram (Table II), corresponding to 18.6 wt % SO_3Na. This would suggest that hydroxide ions are not interacting with every available sulfonic acid group during the titration. Interestingly, some of the larger discrepancies between the NMR wt % SO_3H and the IEC wt % SO_3H were observed for the two batches of S-PPSU obtained from an external supplier, further confirming the subtle dependence of IEC upon microstructure, distribution of sulfonic acids groups along the chain, and small variations in the sulfonation reaction conditions.

Water uptake (at 80°C over 24 h) and proton conductivity were found to increase with increasing IEC and DS, as would be expected for a system in which the number of hydrophilic proton-conducting groups is increasing. Since proton conductivity is highly dependent upon microstructure,[62,63] it has been found that better correlations exist between proton conductivity and IEC than between proton conductivity and purely molecular DS values such as those obtained from NMR spectra.[53] This can be observed in the data of Table II, particularly for the through-plane conductivity values of materials **1** to **4**.

TABLE III
Through-Plane and In-Plane Conductivity, Tensile Strength, Elongation, Water Uptake, and Dimensional Stability Data for Nafion® 212 and for S-PPSU Membranes Formulated with S-POSS, P-POSS, and SA-POSS Nanoadditives, and Having a Range of Sulfonation Levels

Membrane	Conductivity (S cm^{-1})			Tensile strength (N mm^{-2})	Elongation (%)	Water uptake (%)	Dimensional stability (L_c)		
	Through-plane/ 70°C	In-plane/ RT	In-plane/ 80°C				80°C	52% RH	100% RH
Nafion® 212[a] 7.6 wt % SO_3H	0.100	0.100	0.100	25	282	50	−1.20	+2.3	+10.4
100% S-PPSU**3** 20.7 wt % SO_3H IEC = 1.67	0.065	0.049	0.080	33	27	53	−2.27	+0.83	0.0
80% S-PPSU **3** 20% S-POSS	0.083	0.054	0.073	23	36	83	−3.08	+0.58	+1.37
100% S-PPSU **4** 22.2 wt % SO_3H IEC = 1.55	0.038	0.058	–	45	32	54	−1.90	–	+2.70
90% S-PPSU **4** 10% S-POSS	0.068	–	–	39	9	59	−2.20	–	+1.35
80% S-PPSU **4** 20% S-POSS	0.066	–	–	25	4	76	−3.75	–	0.0
100% S-PPSU **2** 23.5 wt % SO_3H IEC = 1.57	0.036	0.069	0.131	44	13	90	−2.33	–	+2.66
90% S-PPSU **2** 10% P-POSS	0.034	0.078	0.128	35	16	85	−3.99	–	+3.09
80% S-PPSU **2** 20% P-POSS	0.059	0.061	0.103	37	14	87	−3.80	–	+1.49
90% S-PPSU **2** 10% SA-POSS	0.072	0.060	0.121	33	38	105	−3.55	–	+3.62
80% S-PPSU **2** 20% SA-POSS	0.042	0.059	0.116	25	28	108	−3.89	–	+4.73

[a] The experimental techniques used to obtain the S-PPSU data in this table were also used to obtain the Nafion® 212 control data.

If a choice of casting solvents is available (in contrast to this study, which was strictly limited to NMP), it should also be noted that casting solvent is crucial to membrane performance and morphology. When sulfonated polyethersulfone (S-PES) membranes were cast from either DMF, DMAc, or NMP, the solvent affected crystallinity and surface energy, which in turn affected IEC, water uptake, and conductivity values.[36] For example, hydrogen-bonding between sulfonic acid groups and residual DMF increased the amorphous character of the membrane and decreased membrane conductivity. Hence, no polymer of a given chemical composition can be said to have a given proton conductivity. Instead proton conductivity is dependent on tertiary microstructure,[62] phase formation and clustering of hydrophilic and hydrophobic moieties,[62,63] and these factors are profoundly influenced by choice of casting solvent.

Preparation and characterization of S-PPSU-POSS membranes

S-PPSU-POSS films were cast from 20 wt % solids NMP solutions (as earlier), but to obtain an S-PPSU-POSS casting solution, it was necessary to dissolve the POSS compounds in water, add the aqueous solution to NMP, and then remove the water to obtain the NMP solution. S-PPSU batches with sulfonation levels between 20.7 and 23.5 wt % SO_3H (materials **2**, **3**, and **4** in Table II) were selected as carrier polymers for the POSS additives because their sulfonation levels were high enough for good proton conductivity, but not so high that the films were at risk of being water soluble. A number of film formulations were cast using S-POSS, P-POSS, or SA-POSS at 10 or 20% loadings. Through- and in-plane proton conductivity, tensile strength, DMA, water uptake, and dimensional stability were measured and compared with Nafion 212 and also with control S-PPSU films containing no additives (Table III). Chemical resistance and leaching issues were also considered, and the morphologies of sample S-POSS, P-POSS, and SA-POSS films were studied by TEM and SEM.

Conductivity

The addition of S-POSS to S-PPSU improved through-plane conductivity relative to the S-PPSU control in all three formulations studied, and

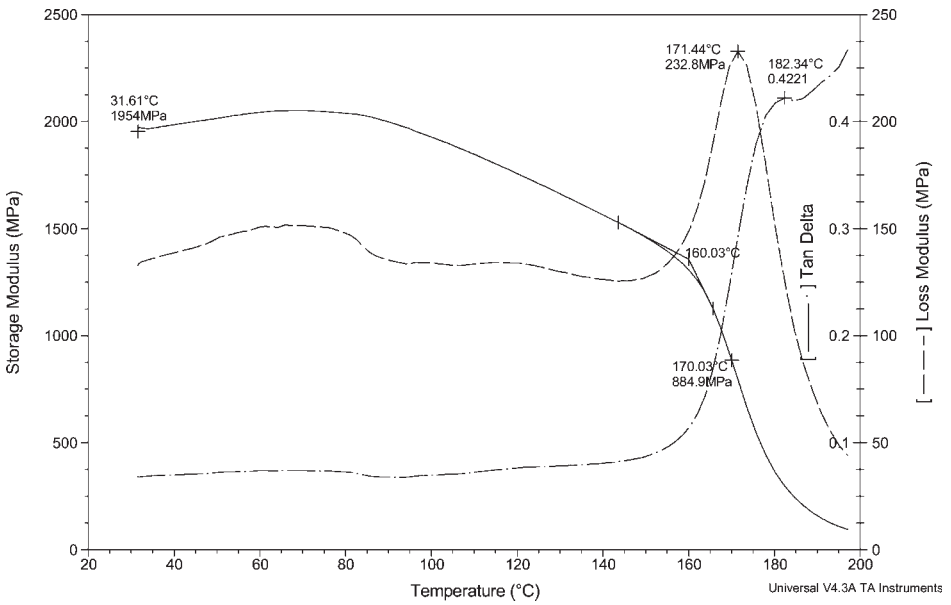

Figure 2 DMA of S-PPSU **4** film.

conductivities comparable to Nafion 212 were obtained. The addition of P-POSS to S-PPSU made a small improvement to through-plane conductivity in the 20% P-POSS formulation, but generally had little impact upon through-plane or in-plane conductivity relative to the control. The addition of SA-POSS to S-PPSU generally improved through-plane conductivity but had little effect on in-plane conductivity. These observations can be rationalized in terms of the smaller domain size of S-POSS versus SA-POSS (see later section on film morphology), and also in terms of the more hydrophobic nature of P-POSS versus S-POSS and SA-POSS (see later section on water uptake). Hence, it appears that the presence of sulfonated POSS additives improves proton conductivity in this system, as it did in the open-cage sulfonated POSS-PVA system reviewed in the Introduction section.[26] However, this system has the advantage of achieving higher proton conductivity at lower sulfonated POSS loadings, e.g., in the open-cage sulfonated POSS-PVA membrane, 0.042 S cm^{-1} was achieved in a 50 wt % POSS formulation,[26] whereas in this S-PPSU system, conductivities of 0.07–0.08 S cm^{-1} are achieved in 10–20 wt % POSS formulations. These results present a contrast to studies of non-proton conducting nanoadditives, which were found to be detrimental to proton conductivity, e.g., 2–10 wt % titanium dioxide nanoparticles (in 100-nm domains) formulated into sulfonated PES (70% DS) caused a dramatic decrease in proton conductivity, from 0.017 S cm^{-1} at 2.5 wt % to 0.002 S cm^{-1} at 12.5 wt % titanium dioxide at 80°C,[14] and the use of 10 nm to 10 μm polysilsesquioxane spheres decreased methanol permeability but also decreased proton conductivity.[24]

Mechanical properties

Pure S-PPSU membranes had tensile strengths far superior to Nafion (33 to 45 N mm^{-2} versus 25 N mm^{-2}, Table III). Although elongations in the S-PPSU systems were lower than Nafion (Table III), no brittle failure was observed. Addition of additives to S-PPSU decreased tensile strength by 5 to 20 N mm^{-2}, with greater decreases generally observed for higher additive levels. In contrast to additive level (10% versus 20%), the identity of the additive (S-POSS, SA-POSS, or P-POSS) had no discernible effect on tensile strength. However, despite these decreases, the tensile strengths of the S-PPSU-POSS films were generally superior to Nafion 212 (23 to 39 N mm^{-2} vs. 25 N mm^{-2}).

Two membranes, 100% S-PPSU **4** and 80% S-PPSU **4** with 20% S-POSS, were characterized by DMA (Figs. 2 and 3). Although the presence of the nanoadditive resulted in a significant decrease in storage modulus at high temperature (170°C), no significant decrease was observed in the 80–120°C range associated with operating fuel cells (Table IV). For comparison, a storage modulus of 600 MPa was measured for Nafion 117 at 30°C, whereas 80% S-PPSU **4** with 20% S-POSS had a storage modulus of 1426 MPa at 30°C.

Water uptake and dimensional stability

The addition of sulfonic acid POSS species (S-POSS and SA-POSS) to S-PPSU resulted in increased water uptake relative to the S-PPSU control, but the addition of P-POSS to S-PPSU resulted in slightly decreased water uptake relative to the S-PPSU

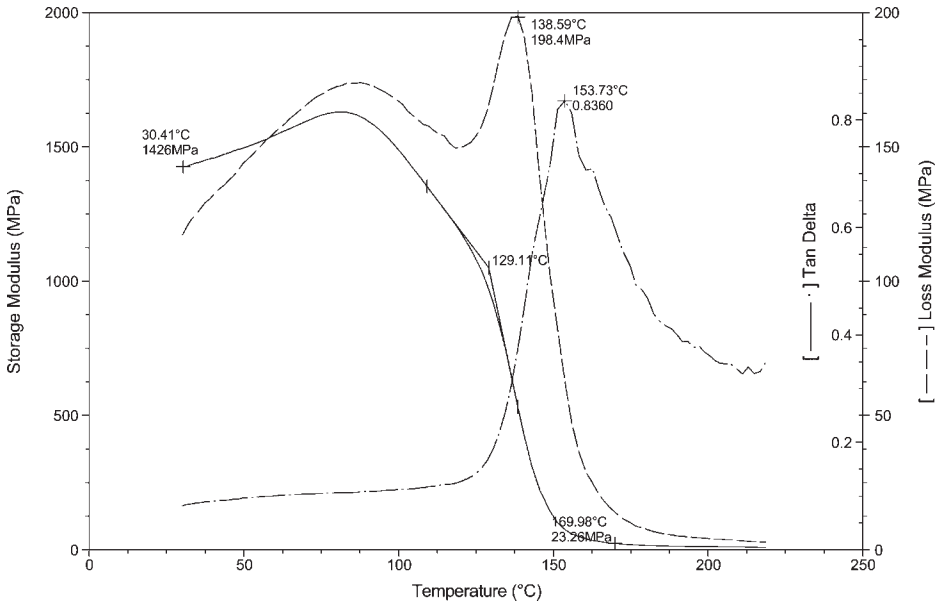

Figure 3 DMA of 80% S-PPSU **4**/20% sulfonated POSS film.

control (because of the less hydrophilic nature of the phosphonic acid half-ester group relative to the sulfonic acid group). In real-world fuel cell applications where the PEM is part of a complex larger assembly of engineering components, high water uptakes become a concern if they cause large volume changes and excessive swelling of the membrane. Hence, the dimensional stability of the membranes was studied using an ASTM method where changes in arcs inscribed on polymer films were measured in varying humidity environments (Table III). Positive L_C values indicate swelling upon hydration, and negative L_C values indicate contraction upon dehydration. All of the S-PPSU and S-PPSU-POSS membranes had superior dimensional stability to Nafion 212 (0–5% L_C for S-PPSU films versus 10% L_C for Nafion 212), despite having much larger water uptake values. Similarly, sulfonated POSS S-PPSU membranes had dimensional stabilities comparable to their S-PPSU controls, despite having larger water uptakes.

Chemical resistance

The proton conductivity, dimensional stability, and mechanical properties discussed earlier suggest that S-PPSU-POSS membranes have great potential in fuel cell applications. However, another key membrane property that must be considered is chemical resistance to acidic conditions and also to oxidative conditions (i.e., attack by peroxide species formed at the fuel cell cathode). Silsesquioxanes are known to be resistant to harsh oxidative and acidic conditions,[25] and aromatic engineering thermoplastics such as Radel R-5000 PPSU are known to have good chemical stability. In one study, Radel R-5000 PPSU was sulfonated *ortho* to the ether oxygen in a conventional electrophilic sulfonation using 96–98% sulfuric acid at 40–60°C, and was also sulfonated *ortho* to the backbone sulfone group via a three-step metallation route involving butyl lithium,[28] and the stabilities and proton conductivities of the two sulfonated polymers were compared. It was found that

TABLE IV
Storage Modulus as a Function of Temperature for Nafion 117®, S-PPSU, and S-PPSU-POSS Films

Membrane	Storage modulus at 30°C (MPa)	Storage modulus at 120°C (MPa)	Storage modulus at 170°C (MPa)
Nafion® 117[a]	600	50	3.3
Sulfonated Radel® R-5000 **4** (22.2 wt % SO_3H)	1,954	1,750	884
80% Sulfonated Radel® R-5000 **4** 20% S-POSS	1,426	1,120	23

[a] The experimental technique used to obtain the S-PPSU data in this table was also used to obtain the Nafion® 117 control data.

sulfonic acid groups *meta* to sulfone had better thermal and chemical stability, and higher proton conductivity than those *ortho* to sulfone and *ortho* to ether, and that o*rtho* ether was the least stable.[28] Despite the relative instability of the sulfonic acid group at the *ortho* ether position (Fig. 1), an S-PPSU membrane has greater chemical stability than the sulfonated-POSS-PVA membrane containing unstable methylene spacer groups discussed earlier.[26]

Leaching

When water-soluble additives such as S-POSS are used in a hydrated membrane, another important issue to consider is leaching, i.e., the loss of the additives from the membrane over time. For example, heteropolyacids have been used in sulfonated PES for fuel cell membranes,[64] but their water solubility can cause them to leach out.[6] Various S-PPSU-POSS membranes were immersed in water at room temperature for 24 h and then dried at 80°C for 2 h. The films were found to have lost 5–10% of their mass. The composition of the lost mass was studied by evaporating the water and analyzing the remaining solid by ^{1}H NMR. Interestingly, this material was found to have no POSS content, but was instead identified as a highly sulfonated S-PPSU (30 wt % SO_3H). Hence it can be concluded that the additives do not leach out of the films under these conditions, but a small fraction of the S-PPSU at the highly sulfonated/water-soluble end of the DS distribution dissolves in the water.

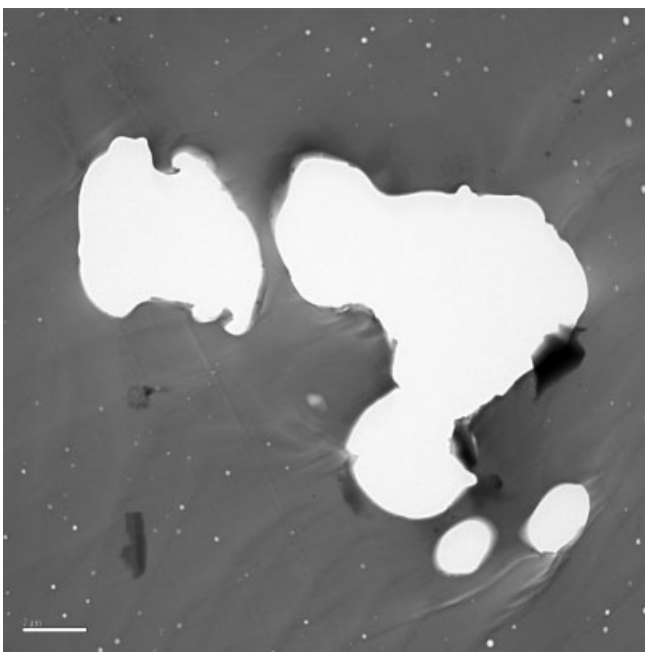

Figure 4 TEM micrograph of 25% S-POSS, 75% sulfonated S-PPSU **1**, scale bar 2 μm.

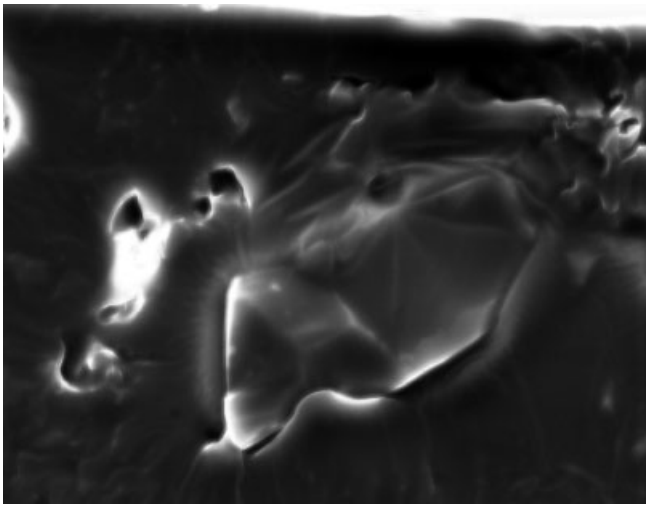

Figure 5 Freeze fracture SEM cross section image through a film of 25% S-POSS and 75% S-PPSU **1**.

Film morphology

TEM studies of the morphology of membranes containing each of the three POSS nanoadditives were carried out. Addition of 1.5-nm POSS additives to membranes resulted in POSS domain sizes of 500 nm and above. A 25% S-POSS/75% S-PPSU **1** (27.2 wt % SO_3H) film, a 20% P-POSS/80% S-PPSU **2** (23.5 wt % SO_3H) film, and a 20% SA-POSS/80% S-PPSU **2** (23.5 wt % SO_3H) film were selected. A TEM study of a 100% S-PPSU **1** (27.2 wt % SO_3H) control film was also carried out. The control film showed no discernible domain structure. In contrast, the sulfonated POSS formulation showed 1–10 μm domains of S-POSS in a continuous S-PPSU matrix phase (Fig. 4). To confirm that the features had a POSS chemical composition, additional SEM experiments were conducted. An SEM X-ray map showed the presence of silicon (POSS) in the 1- to 10-μm sized domains and the absence of silicon in the continuous matrix phase (Figs. 5 and 6). The 20% P-POSS/80% S-PPSU **2** film had a smaller POSS domain size (500 nm to 2 μm, Fig. 7) to the S-POSS/S-PPSU film described earlier. However, the sectioning behavior of the P-POSS/S-PPSU film was very different from that observed for the S-POSS/S-PPSU film. Figure 7 shows that the microtome blade has caused some of the nanoadditive domains to fail cohesively (i.e., particles split across the middle) rather than adhesively (i.e., where the particle matrix interface fails and the particle is ripped cleanly out of the matrix). This suggests either that the interaction between P-POSS molecules in a single domain is weaker or that the interaction between P-POSS and the continuous S-PPSU matrix is stronger.

The 20% SA-POSS/80% S-PPSU **2** film had 2–5 μm POSS domains with a few 6-μm outliers (Fig. 8), comparable to the POSS domains in the S-POSS/

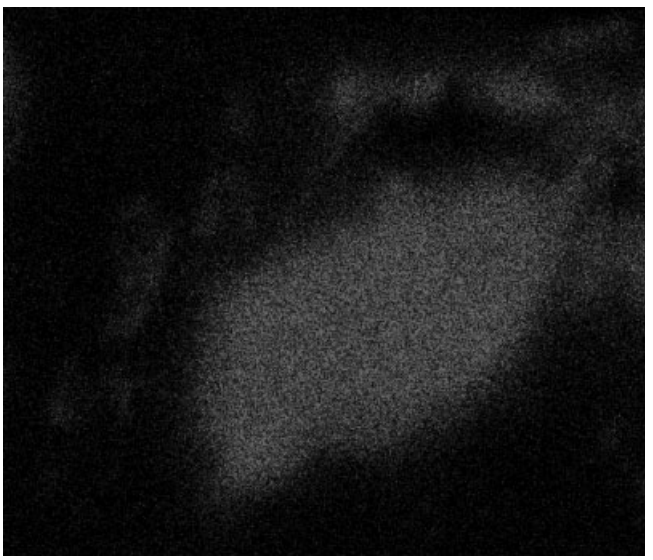

Figure 6 Silicon X-ray map of freeze fracture cross section of Figure 5.

S-PPSU films. This suggests that although the presence of the long-chain alkyl groups improves solubility in organic solvents (as desired), it has little effect upon the dispersion and compatibility of the POSS additive with the sulfonated matrix polymer. The sectioning behavior of this film was the same as that observed for the S-POSS/S-PPSU film. It was also observed that the POSS domains extended out to the edge of the film on one side (left-hand side of Fig. 8) but not on the other (right-hand side of Fig. 8). This could be caused by the tendency of nonpolar alkyl groups to assemble at the air-solution interface of the

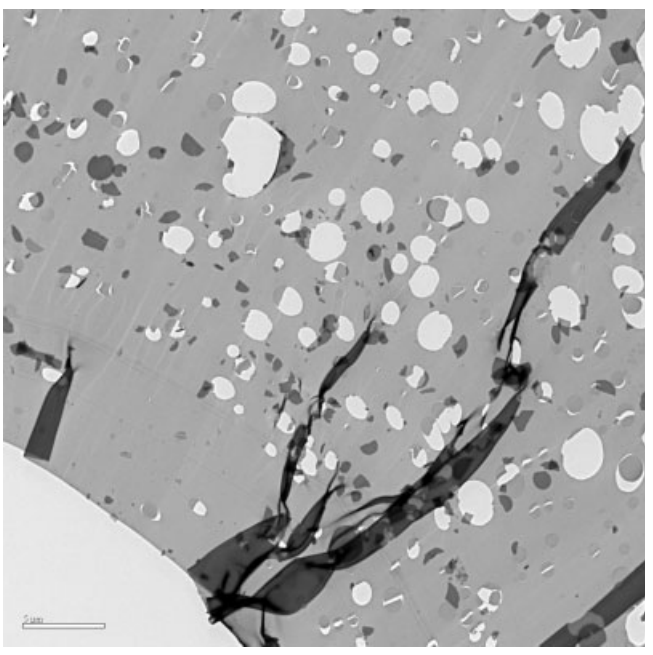

Figure 7 TEM image of a cross section of 20% P-POSS/80% S-PPSU **2** (scale bar, 5 μm).

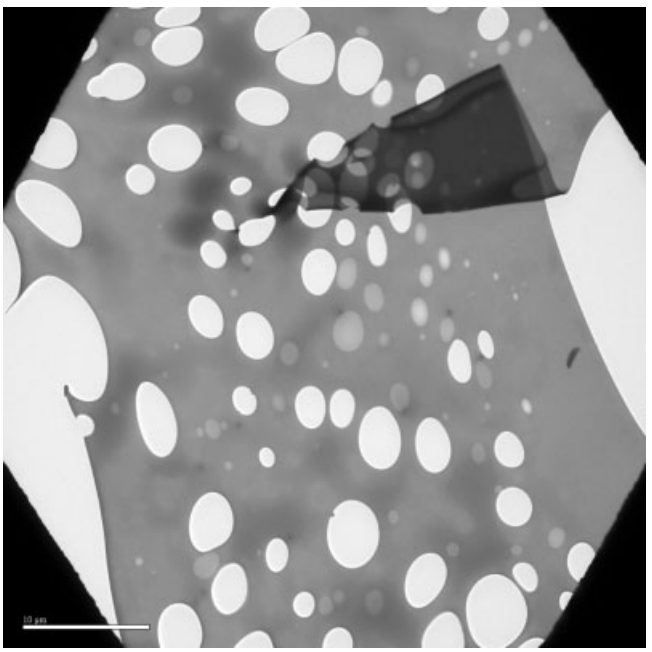

Figure 8 TEM image of a cross section of 20% SA-POSS/80% S-PPSU **2** (scale bar, 10 μm).

film-casting solution during film fabrication. This illustrates that even films that are designed to be homogenous and isotropic may turn out to be anisotropic in reality. Hence conductivity values should be quoted with caution and with the awareness that in-plane and through-plane values (measured in directions at right angles to each other) may differ.

CONCLUSIONS

POSS carrying sulfonic acid groups (S-POSS), a mixture of sulfonic acid and octadecyl groups (SA-POSS), and phosphonic acid half-ester groups (P-POSS) were synthesized and fully characterized. Eight batches of sulfonated Radel R5000 S-PPSU carrier polymers of varying DS were prepared in chlorosulfonic acid/acetic anhydride aromatic electrophilic sulfonation reactions. S-PPSU batches containing 20.7–23.5 wt % SO_3H were selected as carrier polymers for the POSS nanoadditives because their sulfonation levels were high enough for good conductivity, but not high enough to result in water solubility. A number of S-PPSU-POSS films were cast from NMP with POSS loadings of 10 or 20%, and through-plane and in-plane proton conductivity, tensile strength, storage modulus, water uptake, dimensional stability, and leaching behavior were studied. When compared with Nafion, the S-POSS/S-PPSU composite membranes exhibited comparable proton conductivity in combination with superior dimensional stability and mechanical strength. When compared with control S-PPSU membranes, the composite S-POSS/S-PPSU membranes exhibited

superior conductivity, comparable dimensional stability, and slightly decreased mechanical strength. The presence of POSS nanoadditives increased water uptake relative to S-PPSU control films, but no swelling or decrease in dimensional stability was observed at higher water uptakes. Leaching experiments on membranes resulted in small mass losses caused by the dissolution of a small fraction of highly sulfonated water-soluble S-PPSU (30 wt % SO_3H) rather than the loss of any POSS additive. TEM showed that the S-POSS/S-PPSU membrane had 1–10 μm POSS domains, the SA-POSS/S-PPSU membrane had 2–5 μm POSS domains, and the P-POSS/S-PPSU membrane had 500 nm to 2 μm POSS domains. SEM X-ray mapping showed that silicon was present in the domain structures, but not in the continuous matrix, confirming that the domain structures contained POSS. The SA-POSS/S-PPSU membrane was observed to be anisotropic, having POSS domains close to the surface on one side but not on the other, and illustrating the importance of obtaining both through-plane and in-plane conductivity measurements. The high proton conductivities, and excellent dimensional stabilities and mechanical properties of S-PPSU-POSS composite membranes in combination with their known resistance to acidity, oxidizing environments, and leaching, make them very promising alternatives to Nafion as fuel cell proton exchange membrane materials.

The authors thank Matthew Stephenson and Kevin Battjes of Impact Analytical (Midland, MI) for carrying out the microscopy portion of this study, Xiaodong Liu of Impact Analytical for performing the DMA experiments, and Ryszard Wycisk of Case Western Reserve University (Cleveland, OH) for measuring in-plane proton conductivity.

References

1. Hickner, M. A.; Ghassami, H.; Kim, Y. S.; Einsla, B. B.; McGrath, J. E. Chem Rev 2004, 104, 4587.
2. Iojoiu, C.; Marechal, M.; Chabert, F.; Sanchez, Y. J. Y. Fuel Cells 2005, 5, 344.
3. Formato, R. M.; Kovar, R. F.; Osenar, P.; Landrau, N. (Foster Miller, Inc.). WO Pat. 99/10165 (1999).
4. Formato, R.; Kovar, R.; Osenar, P.; Landrau, N.; Rubin, L. (Foster-Miller Inc.). U.S. Pat. 7,052,793 B2 (2006).
5. Bahar, B.; Hobson, A. R. (Gore Associates). U.S. Pat. 5,635,041 (1997).
6. Li, L.; Wang, Y. J Power Sources 2006, 162, 541.
7. Costamagna, P.; Yang, C.; Bocarsly, A. B.; Srinivasan, S. Electrochim Acta 2002, 47, 1023.
8. Park, Y. S.; Yamazaki, Y. Solid State Ionics 2005, 176, 1079.
9. Miyake, N.; Wainright, J. S.; Savinell, R. P. J Electrochem Soc 2001, 148, A905.
10. Shao, Z.-G.; Joghee, P.; Hsing, I.-M. J Membr Sci 2004, 229, 43.
11. Lin, C. W.; Thangmuthu, R.; Chang, P. H. J Membr Sci 2005, 254, 197.
12. Antonucci, P. L.; Ario, A. S.; Creti, P.; Ramunni, E.; Antonucci, V. Solid State Ionics 1997, 125, 431.
13. Adjemian, K. T.; Lee, S. J.; Srinivasan, S.; Benziger, J.; Bocarsly, A. B. J Electrochem Soc 2002, 149, A256.
14. Prashantha, K.; Park, S. G. J Appl Polym Sci 2005, 98, 1875.
15. Su, Y. H.; Liu, Y. L.; Sun, Y. M.; Lai, J. Y.; Guiver, M. D.; Gao, Y. J Power Sources 2006, 155, 111.
16. Chang, H. Y.; Lin, C. W. J Membr Sci 2003, 218, 295.
17. Wilson, B. C.; Jones, C. W.; Macromolecules 2004, 37, 9709.
18. Kim, D.; Scibioh, A.; Kwak, S.; Oh, I.-H.; Ha, H. Y. Electrochem Commun 2004, 6, 1069.
19. Acosta, J. L.; Gonzalez, L.; Ojeda, M. C.; del Rio, C. J Appl Polym Sci 2003, 90, 2715.
20. Holmberg, B. A.; Wang, H.; Norbeck, J. M.; Yan, Y. Polym Prepr 2004, 45, 24.
21. Lee, J.; Mah, S.; Jung, J.; Lee, J.; Kim, D. U.S. Pat. 0,190,385 A1 (2007).
22. Karthikeyan, C. S.; Nunes, S. P.; Schulte, K. Macromol Chem Phys 2006, 207, 336.
23. Kim, Y. B.; Kim, Y. A.; Yoon, K. S. Macromol Rapid Commun 2006, 27, 1247.
24. Cheon, H. S.; Hong, S. U.; Kim, Y. B.; Park, H. H. Memburein 2005, 15, 1.
25. Khiterer, M.; Loy, D. A.; Cornelius, C. J.; Fujimoto, C. H.; Small, J. H.; McIntire, T. M.; Shea, K. J. Chem Mater 2006, 18, 3665.
26. Chang, Y.-W.; Wang, E.; Shin, G.; Han, J.-E.; Mather, P. T. Polym Adv Technol 2007, 18, 535.
27. Stoler, E. J.; Nair, B. R.; Kovar, R. F.; Ofer, D. Thirty Sixth Proceedings of the Intersociety Energy Conversion Engineering Conference; Society of Automotive Engineers: Warrendale, Pennsylvania; 2001; Vol. 2, p 975.
28. Xing, D.; Kerres, J. Polym Adv Technol 2006, 17, 591.
29. Dyck, A.; Fritsch, D.; Nunes, S. P. J Appl Polym Sci 2002, 86, 2820.
30. Mottet, C.; Revillon, A.; Le Perchec, P.; Llauro, M. F.; Guyot, A. Polym Bull 1982, 8, 511.
31. Bell, C. M.; Deppisch, R.; Gohl, H. J. (Gambro Dialysatoren GmbH & Co.). U.S. Pat. 5,401,410 (1995).
32. Sun, H.; Venkatasubramanian, N.; Houtz, M. D.; Mark, J. E.; Arnold, F. E. Polym Prepr 2002, 43, 471.
33. Blanco, J. F.; Nguyen, Q. T.; Schaetzel, P. J Membr Sci 2001, 186, 267.
34. Guan, R.; Zou, H.; Lu, D.; Gong, C.; Liu, Y. Eur Polym Mater 2005, 41, 1554.
35. Guan, R.; Dai, H.; Li, C.; Liu, J.; Xu, J. J Membr Sci 2006, 277, 148.
36. Lu, D.; Zou, H.; Guan, R.; Dai, H.; Lu, L. Polym Bull 2005, 54, 21.
37. Bae, T.-H.; Kim, I.-C.; Tak, T.-M. J Membr Sci 2006, 275, 1.
38. Kim, I. C.; Choi, J. G.; Tak, T. M. J Appl Polym Sci 2046, 1999, 74.
39. Ghosh, A. K.; Ramachandhran, V.; Hanra, M. S.; Misra, B. M. J Macromol Sci Pure Appl Chem 2002, A39, 199.
40. Cui, W.; Socza-Guth, T.; Frank, G. (Celanese Ventures GmbH). U.S. Pat. 6,790,931 B2 (2004).
41. Coplan, M. J.; Gotz, G. (Albany International Corp.). U.S. Pat. 4,413,106 (1983).
42. Buck, C. J. (Johnson and Johnson). U.S. Pat. 430,513 (1982).
43. Byun, I. S.; Kim, I. C.; Seo, J. W. J Appl Polym Sci 2000, 76, 787.
44. Ditter, J. F.; Hoffman, C. S. (Memtec America Co.). WO Pat. 9726284-A1 (1997).
45. Brousse, C. L.; Chapurlat, R.; Quentin, J. P. Desalination 1976, 18, 137.
46. Blanco, J. F.; Sublet, J.; Nguyen, Q. T.; Schaetzel, P. J Membr Sci 2006, 283, 27.
47. Li, L.; Wang, Y. J Membr Sci 2005, 246, 167.
48. Hung, J.; Zhou, H.; Moore, D. R.; Harmon, M. E.; Brunelle, D. J.; Liu, H. (General Electric Co.). U.S. Pat. 142,613 (2007).
49. Manea, C.; Mulder, M. Desalination 2002, 147, 179.

50. Parcero, E.; Herrera, R.; Nunes, S. P. J Membr Sci 2006, 285, 206.
51. Di Vona, M. L.; D'Epifanio, A.; Marani, D.; Trombetta, M.; Traversa, E.; Licoccia, S. J Membr Sci 2006, 279, 186.
52. Brick, C. M.; Tamaki, R.; Kim, S. G.; Asuncion, M. Z.; Roll, M.; Nemoto, T.; Ouchi, Y.; Chujo, Y.; Laine, R. M. Macromolecules 2005, 38, 4655.
53. Schuster, M.; Kreuer, K.-D.; Andersen, H. T.; Maier, J. Macromolecules 2007, 40, 598.
54. Guiver, M. D.; Kutowy, O. (National Research Council of Canada). U.S. Pat. 4,996,271 (1991).
55. Lide, D. R. CRC Handbook of Chemistry and Physics, 72nd ed.; CRC Press: Boca Raton, FL, 1991-1992; pp 15–21.
56. Fieser, L. F.; Fieser, M. Reagents for Organic Synthesis; Wiley: New York, 1967; Vol. 1, p 26.
57. Allcock, H. R.; Hofmann, M. A.; Wood, R. M. Macromolecules 2001, 34, 6915.
58. Lafitte, B.; Jannasch, P. J. Polym Sci A, Polym Chem 2005, 43, 273.
59. Allcock, H. R.; Hofmann, H. R.; Ambler, C. M.; Morford, R. V. Macromolecules 2002, 35, 3484.
60. Colthrup, N. B.; Daly, L. H.; Wiberly, S. E. Introduction to Infrared and Raman Spectroscopy; Academic Press: San Diego, 1990; p 364.
61. Pouchert, C. J.; Behnke, J. The Aldrich Library of ^{13}C and ^{1}H NMR Spectra; Aldrich Chem Company: USA, 1993; Vol. 2, p 1694.
62. Ma, C.; Zhang, L.; Mukerjee, S.; Ofer, D.; Nair, B. J Membr Sci 2003, 219, 123.
63. Kreuer, K. D. Solid State Ionics 2000, 149, 136.
64. Hung, J.; Zhou, H.; Brunelle, D. J.; Harmon, M. E.; Steigler, D.; Liu, H.; Moore, D. R. (General Electric Co). U.S. Pat. 100131 (2007).